Supplement of Atmos. Chem. Phys., 17, 1805–1828, 2017
http://www.atmos-chem-phys.net/17/1805/2017/
doi:10.5194/acp-17-1805-2017-supplement

Atmospheric Chemistry and Physics
Open Access

Supplement of

Differences in BVOC oxidation and SOA formation above and below the forest canopy

Benjamin C. Schulze et al.

Correspondence to: Robert J. Griffin (rob.griffin@rice.edu)

Table S1. Description of values used in calculation of deposition velocities of particles and gases[1]. H indicates Henry's Law Coefficient, f_o is the reactivity factor, and MCM species indicates to which compounds (or classes of compounds) the parameters were applied.

Name	Diffusivity ($m^2\ s^{-1}$)	H ($M\ atm^{-1}$)	f_o	MCM Species
H2O2	1.75×10^{-5}	1.1×10^{5}	1	Hydrogen Peroxide
Formic	1.34×10^{-5}	5.6×10^{3}	0	Formic Acid
HNO3	1.15×10^{-5}	3.2×10^{5}	1	Nitric Acid
HMHP	1.14×10^{-5}	1.3×10^{6}	0.1	Hydroxymethylhydroperoxide
HAC	1.06×10^{-5}	2.0×10^{3}	0	Hydroxyacetone
PAA	1.04×10^{-5}	5.2×10^{2}	0.1	Peroxyacetic acid
HDC4	9.01×10^{-6}	2.0×10^{3}	0	C_4 Hydroxy dicarbonyls
DHC4	8.92×10^{-6}	2.0×10^{3}	0	C4 Dihydroxy carbonyls
HPALD	8.45×10^{-6}	4.0×10^{4}	0	Isoprene hydroperoxyaldehyde
ISOPOOH/IEPOX	8.37×10^{-6}	4.0×10^{4}	0	Isoprene hydroxy-hydroperoxide and epoxides
PROPNN	8.34×10^{-6}	1.0×10^{4}	0	Propanone nitrate
ISOPN	7.50×10^{-6}	5.0×10^{3}	0	Isoprene hydroxy nitrates
MACN/MVKN	7.45×10^{-6}	6.0×10^{3}	0	Methacrolein and Methyl vinyl ketone hydroxy nitrates
INP	7.12×10^{-6}	5.0×10^{3}	0	Isoprene nitrooxy hydroperoxides
MTNP	5.98×10^{-6}	1.0×10^{3}	0	Monoterpene nitrooxy hydroperoxides
ANIT[2]	5.98×10^{-6}	1.0×10^{3}	0	Other monoterpene nitrates
OTHER[2]	5.98×10^{-6}	1.0×10^{3}	0	Other α-pinene products
ISOPOOH2[3]	8.37×10^{-6}	1.0×10^{4}	0	Other isoprene hydroperoxides
ISOPNIT[4]	7.12×10^{-6}	5.0×10^{3}	0	Other isoprene nitrates
ISOPOTHER[4]	7.12×10^{-6}	5.0×10^{3}	0	Other isoprene oxidation products
RAD[5]	0	0	0	Alkoxy and peroxy radicals.
MACR[6]	5.02×10^{-5}	6.5×10^{0}	1	Methacrolein
MVK[6]	5.02×10^{-5}	4.1×10^{1}	1	Methyl vinyl ketone
CH3CHO[6]	7.12×10^{-6}	1.5×10^{1}	0	Acetaldehyde
GLY	4.49×10^{-5}	4.1×10^{4}	0	Glyoxal
PAN[6]	7.02×10^{-5}	5.0×10^{0}	0.1	Peroxyacetylnitrates
ACETOL[6]	7.12×10^{-6}	2.4×10^{6}	1	Acetone Alcohol
HCHO[6]	3.43×10^{-5}	2.3×10^{4}	1	Formaldehyde
N2O5[6]	5.81×10^{-5}	1×10^{20}	1	Dinitrogen Pentoxide

[1]Unless otherwise indicated, values obtained from Nguyen et al. (2015).
[2]Values assumed the same as MTNP.
[3]Values assumed the same as ISOPOOH.
[4]Values assumed the same as INP.
[5]Radical species assumed to undergo negligible deposition.
[6]Diffusivity values obtained from Ashworth et al. (2015). Henry's Law coefficients obtained from Sander et al. (1999). Reactivity factor of MACR and MVK adjusted to 1 in accordance with findings of Karl et al. (2010).

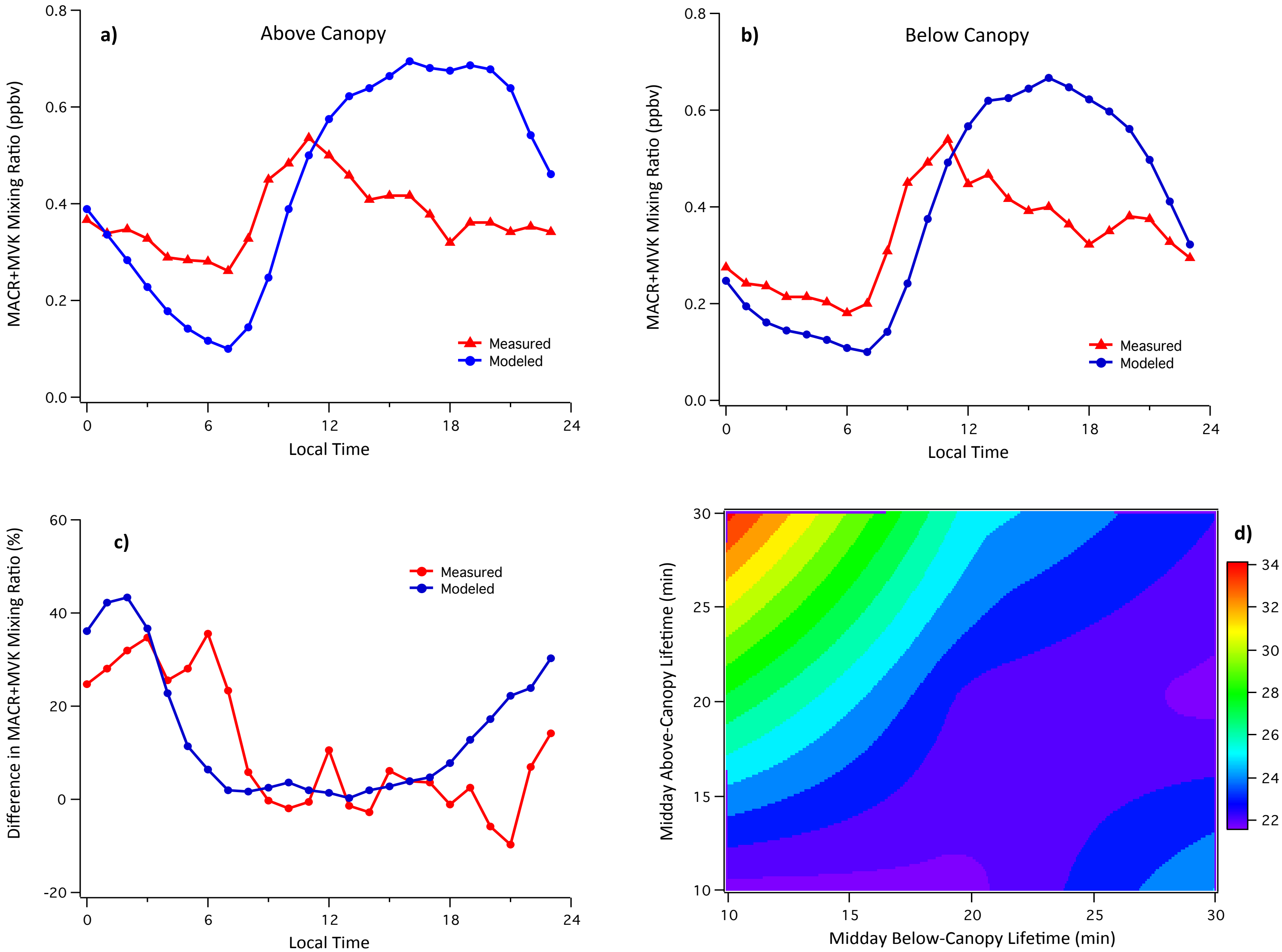

Figure S1. Comparison of above-canopy **(a)** and below-canopy **(b)** median MACR+MVK measurements during CABINEX 2009 to 0D model predictions. **(c)** Comparison of the measured and modeled differences (%) in MACR+MVK mixing ratios between the above-canopy and below-canopy environments. Positive values indicate higher concentrations above the canopy than below. **(d)** Cost function output for analysis of different above and below canopy lifetimes with respect to transport. Smaller values indicate better agreement with measured concentrations.

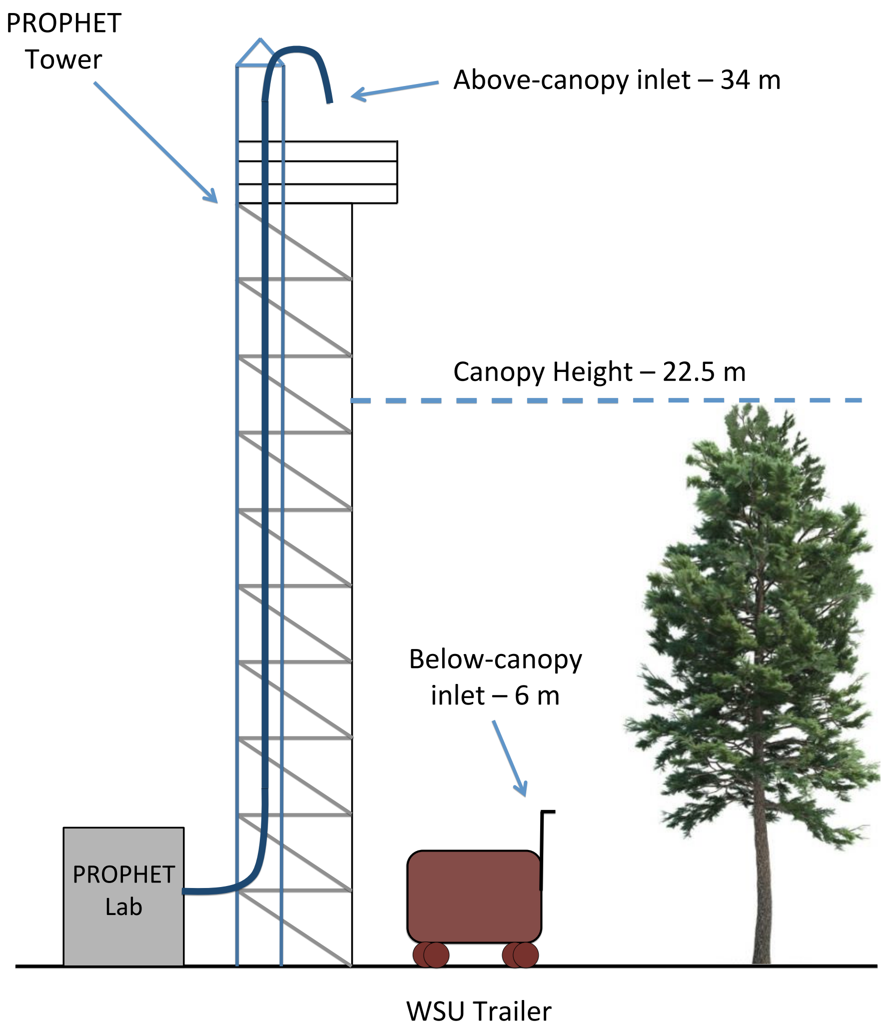

Figure S2. Depiction of the PROPHET tower and inlet locations used during CABINEX 2009.

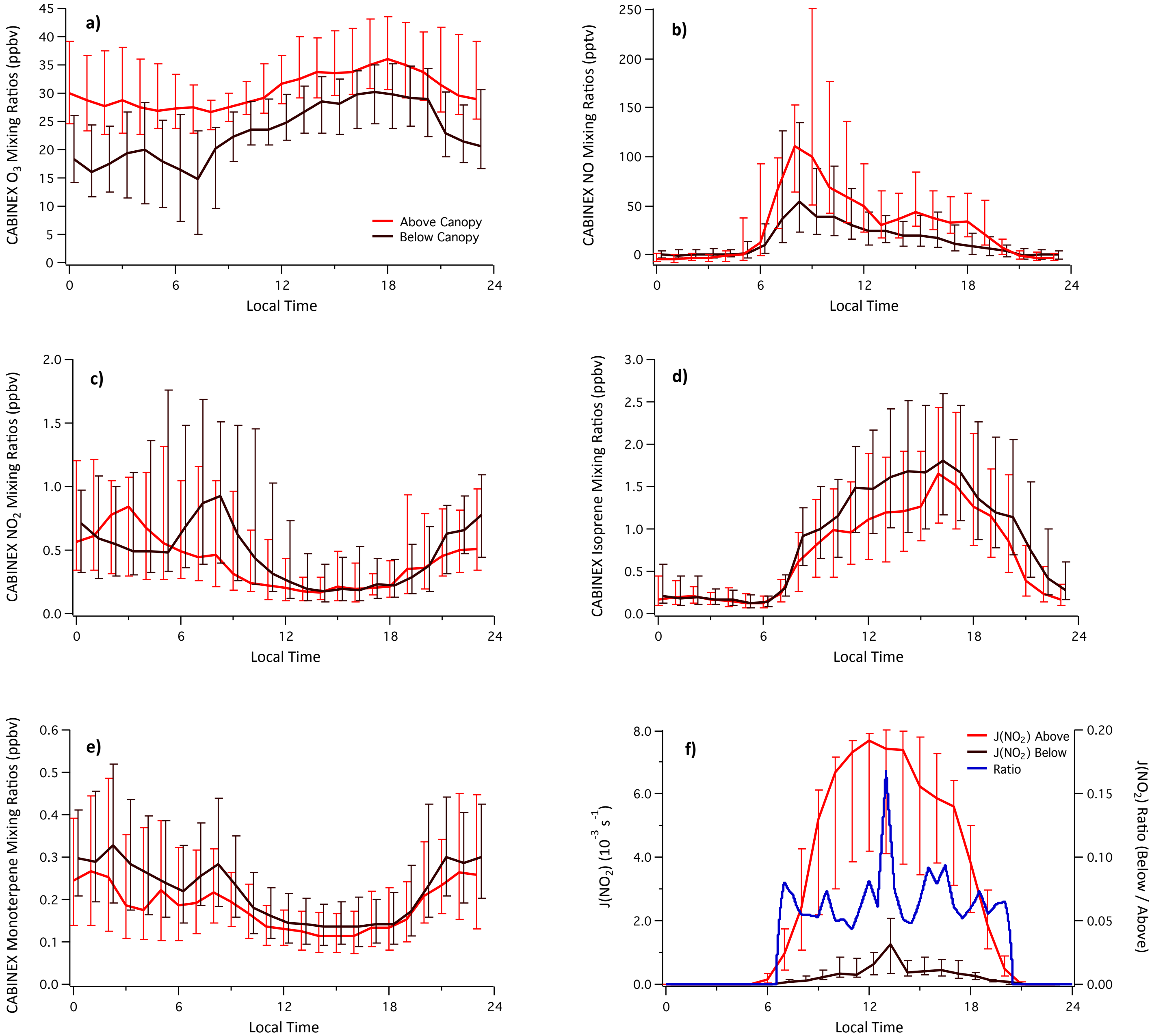

Figure S3. CABINEX 2009 measurements of ambient **(a)** O_3 (ppbv), **(b)** NO (pptv), **(c)** NO_2 (ppbv), **(d)** isoprene (ppbv), **(e)** monoterpenes (ppbv), and **(f)** the photolysis rate of NO_2 (JNO_2) (10^{-3} s^{-1}). Lighter (red) colored lines indicate above-canopy measurements; darker-colored (black) lines indicate below-canopy measurements. Solid lines represent median measured values, while upper and lower bars represent 75^{th} and 25^{th} percentiles respectively. Below-canopy values have been offset by 15 minutes to aid interpretation.

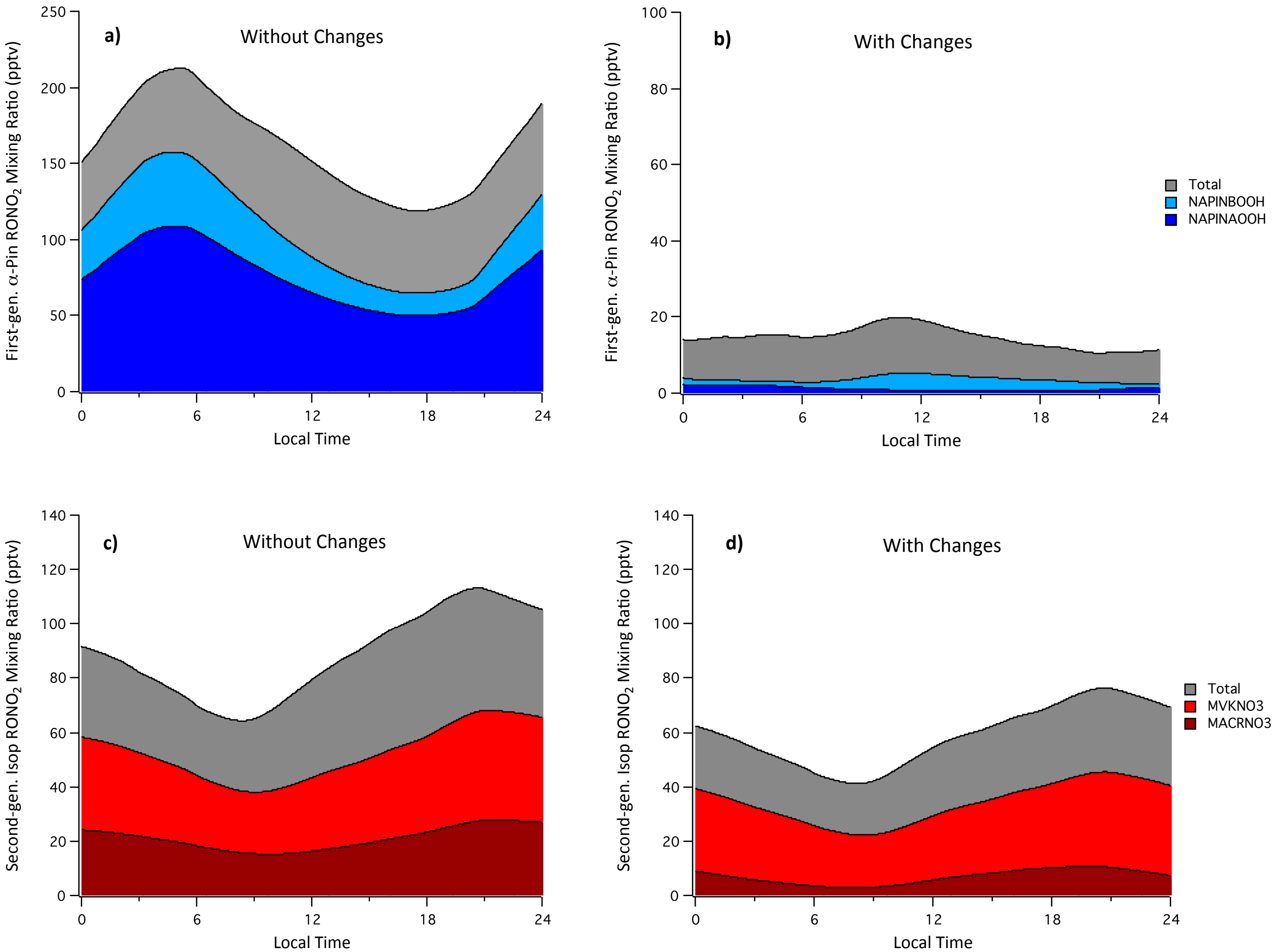

Figure S4. Concentrations of major $RONO_2$ products from α-pinene **(a,b)** and isoprene **(c,d)** above the canopy without (left) and with (right) the changes to the chemical mechanism described in Section 2.6.

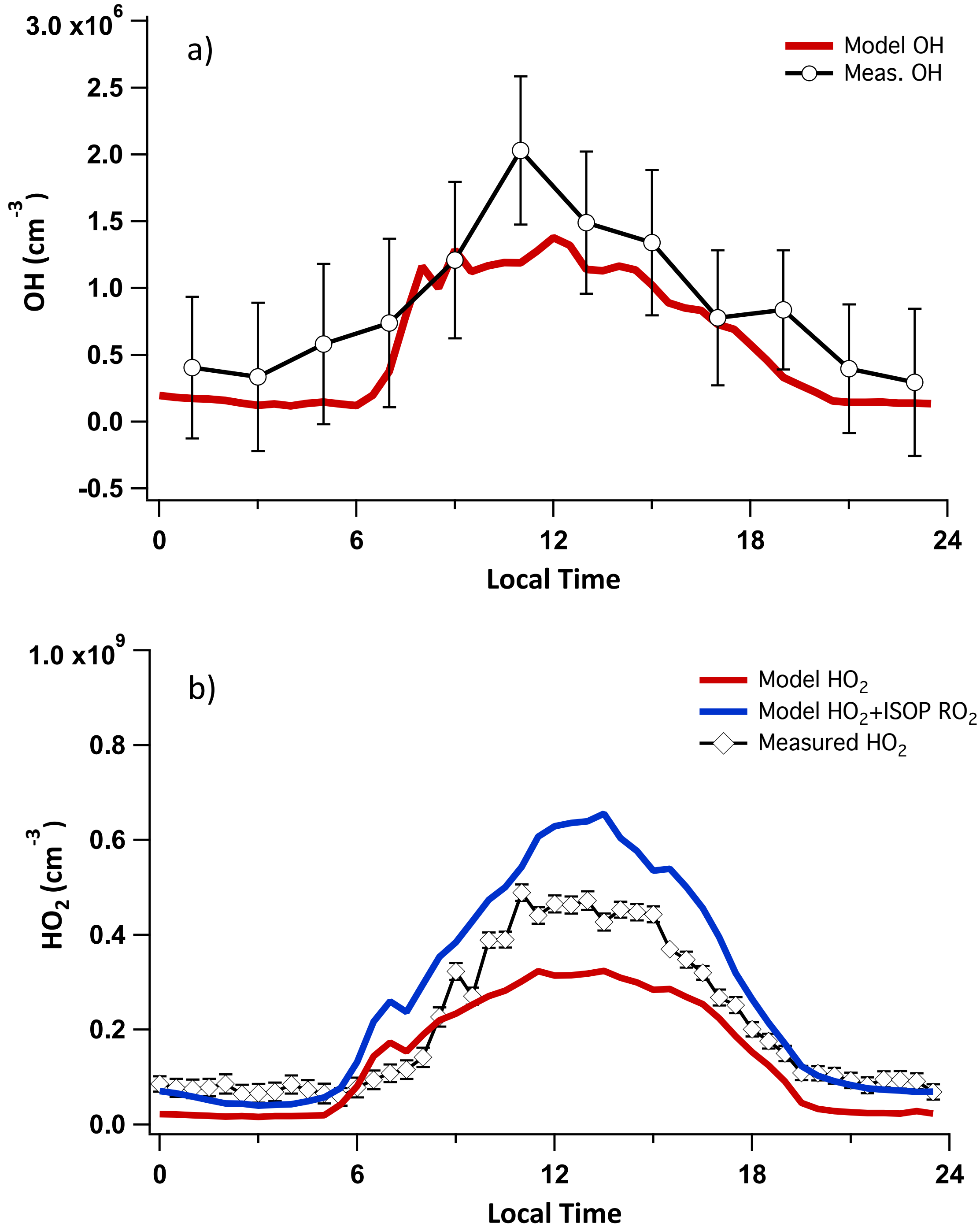

Figure S5. (a) Comparison of above-canopy median OH measurements during CABINEX 2009 to 0D model predictions for the ambient CABINEX model scenario. **(b)** Comparison of above-canopy median HO_2 measurements during CABINEX 2009 to 0D model predictions of HO_2 and HO_2 + isoprene RO_2 for the ambient CABINEX model scenario. Error bars indicate median measurement precision.

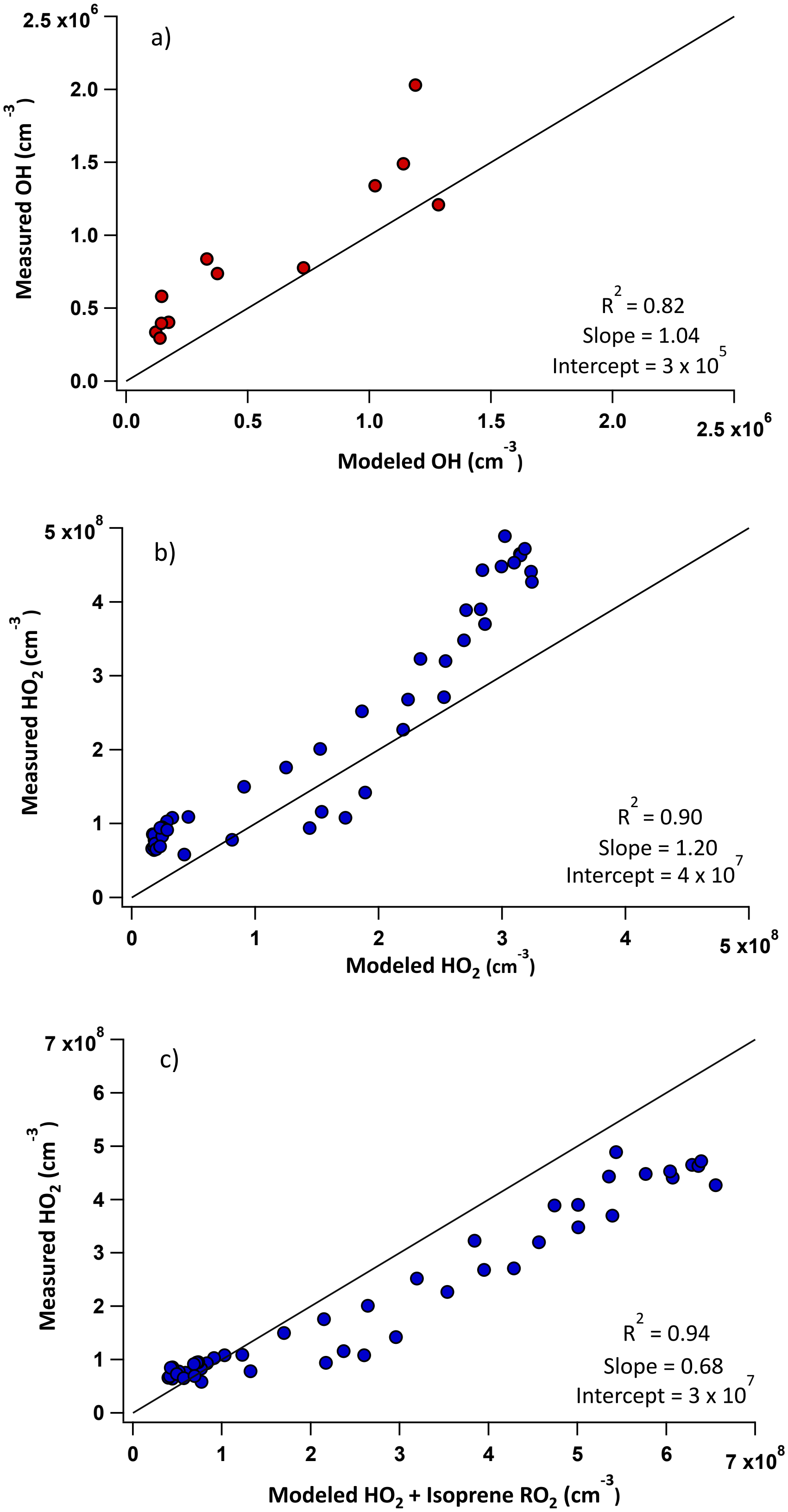

Figure S6. Linear regression of **(a)** median OH measurements during CABINEX 2009 and 0D model predictions, **(b)** median HO_2 measurements and 0D model predictions, and **(c)** median HO_2 measurements and HO_2 + isoprene RO_2 0D model predictions. The 1:1 line is included in each plot for reference.

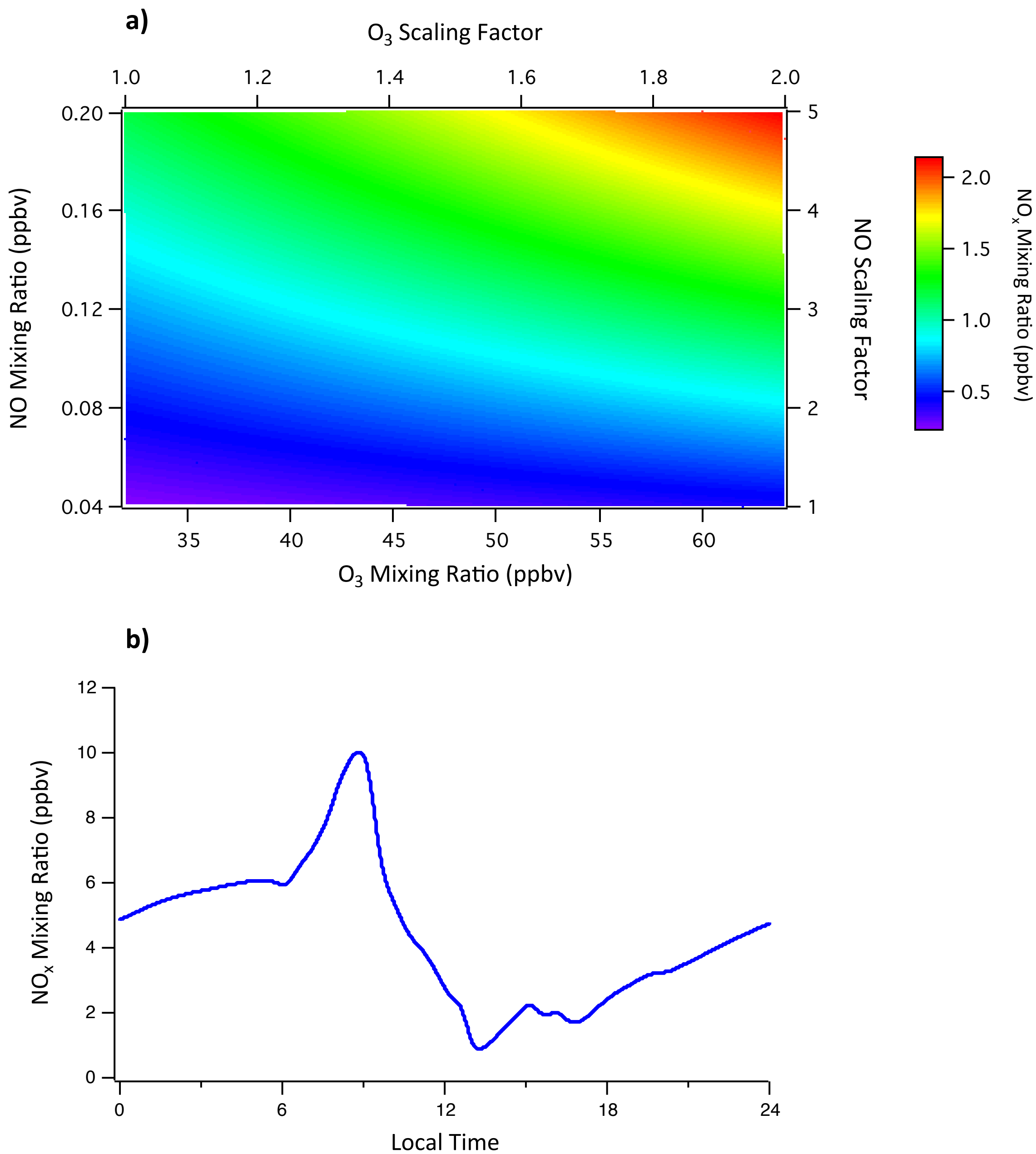

Figure S7. (a) Average NO_x mixing ratio above the canopy from 11:00-15:00 as a function of NO and O_3 mixing ratios **b)** Diurnal profile of total above-canopy NO_x for the most polluted sensitivity test (diurnal profiles of O_3 and NO scaled by factors of 2 and 5, respectively).

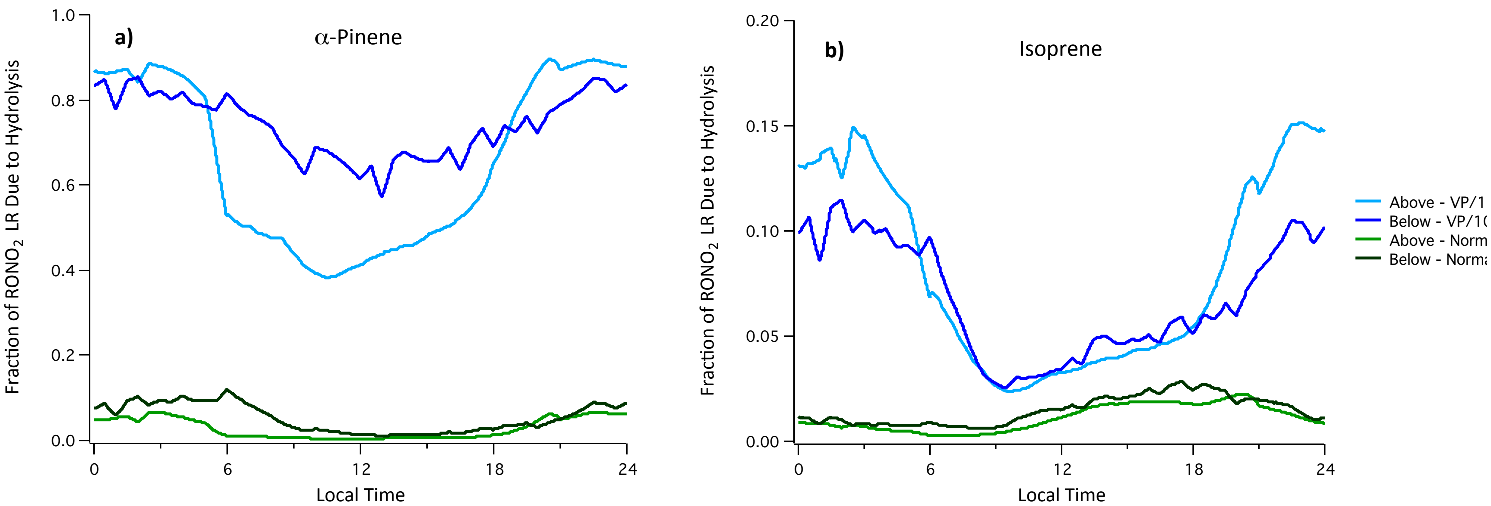

Figure S8. (a) Fraction of total α-pinene $RONO_2$ loss rate due to heterogeneous hydrolysis. Green lines represent a scenario using vapor pressures as calculated by the SIMPOL.1 method, while blue lines represent a scenario with all vapor pressures decreased by a factor of 100. Lighter-colored lines indicate above-canopy conditions; darker-colored lines indicate below-canopy conditions. **(b)** Same as (a), but for isoprene $RONO_2$. Note the different y-axes. Only tertiary isoprene nitrates are assumed to undergo hydrolysis in the model, whereas all α-pinene nitrates hydrolyze.

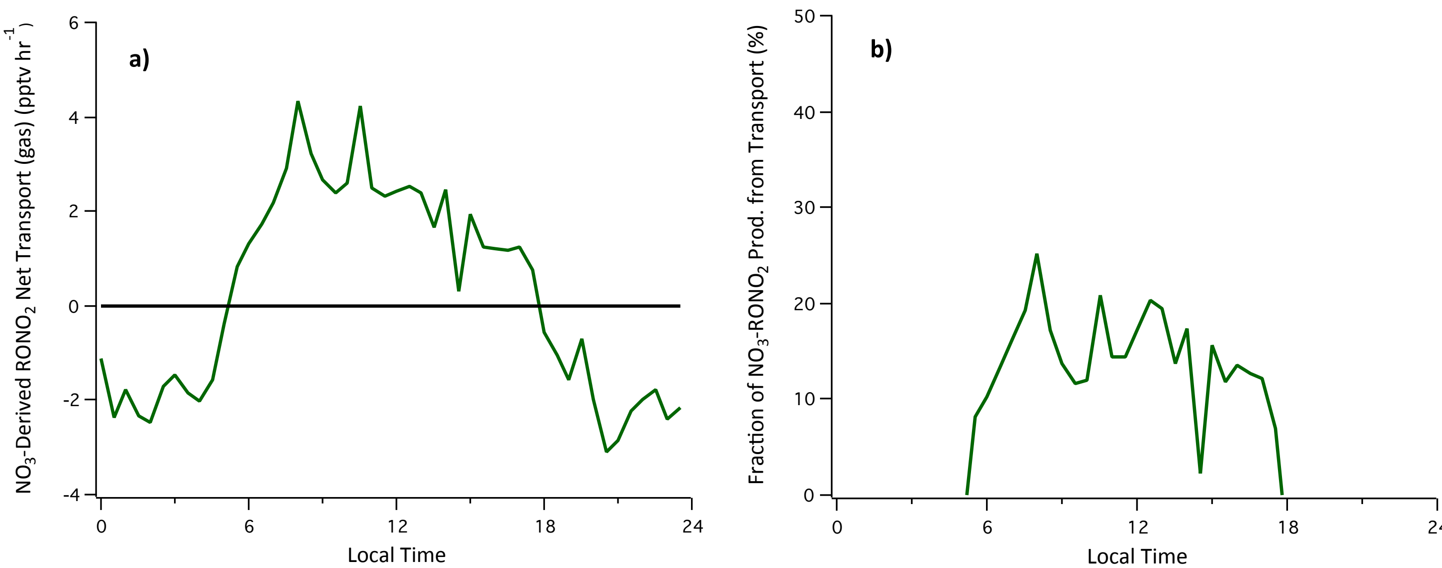

Figure S9. a) Net transport of NO_3-derived $RONO_2$ above the canopy assuming all oxidation product vapor pressures are reduced by a factor of 100. Positive indicates transport from the below-canopy environment; negative indicates transport to the below-canopy environment. **b)** Percent of total NO_3-derived $RONO_2$ production contributed by net transport from the below-canopy environment in this scenario.

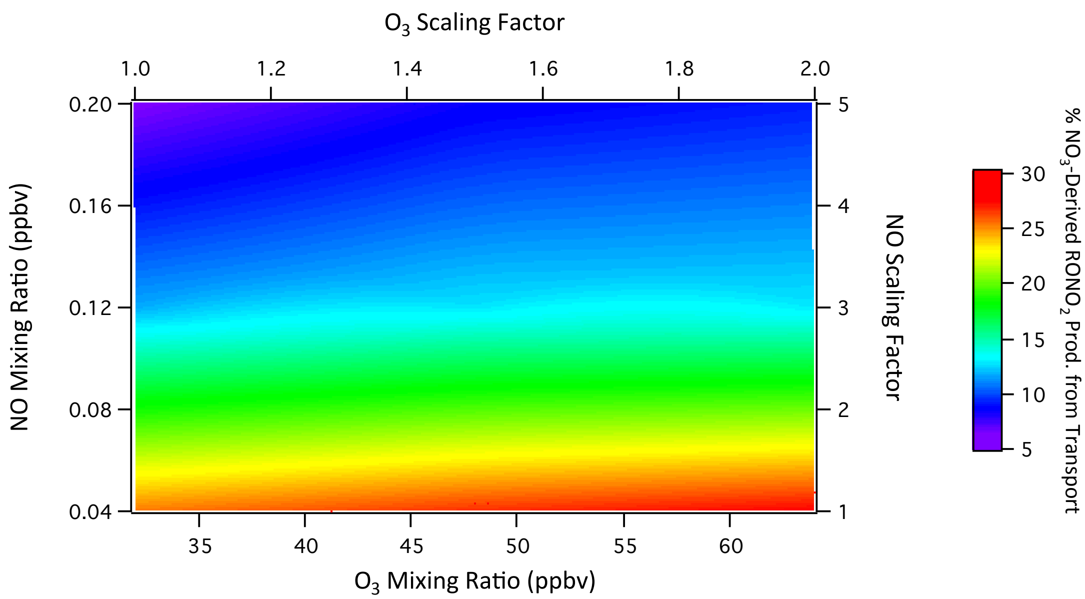

Figure S10. Percent of total NO_3-derived $RONO_2$ production contributed by net transport from the below-canopy environment as a function of O_3 and NO mixing ratios. Values represent averages from 11:00 to 15:00.

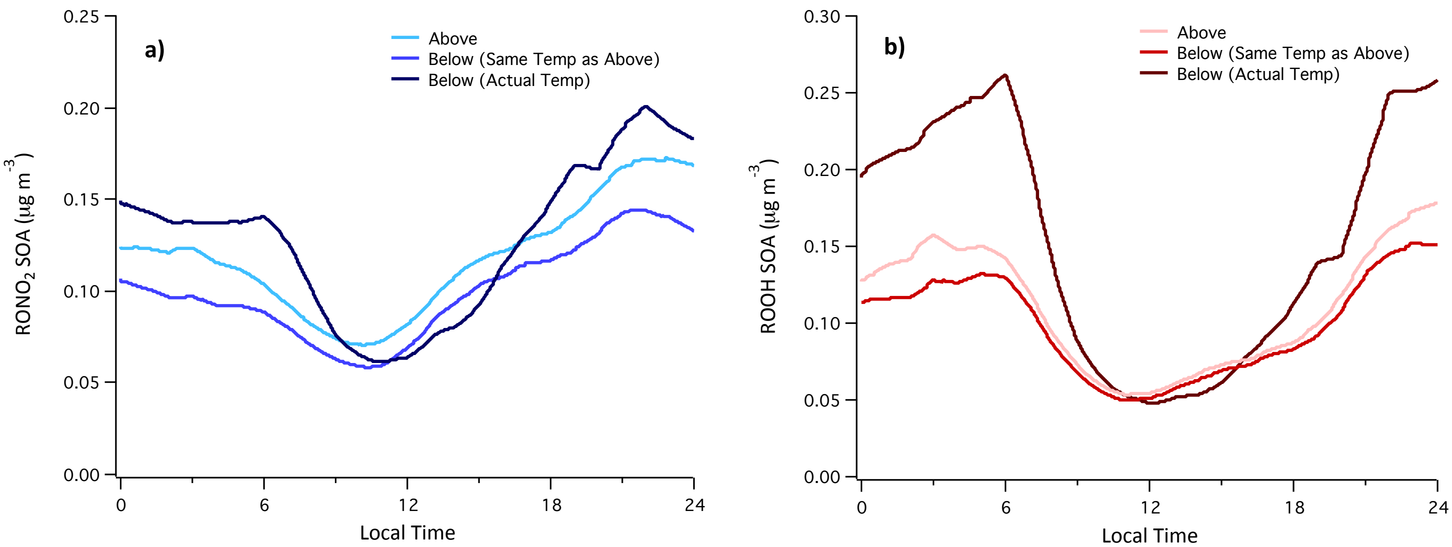

Figure S11. Effect of temperature on semi-volatile SOA formation from **(a)** $RONO_2$ oxidation products and **(b)** ROOH oxidation products. The line of intermediate color in each plot (i.e. "medium" darkness) notes the scenario using the same temperature above and below the canopy.

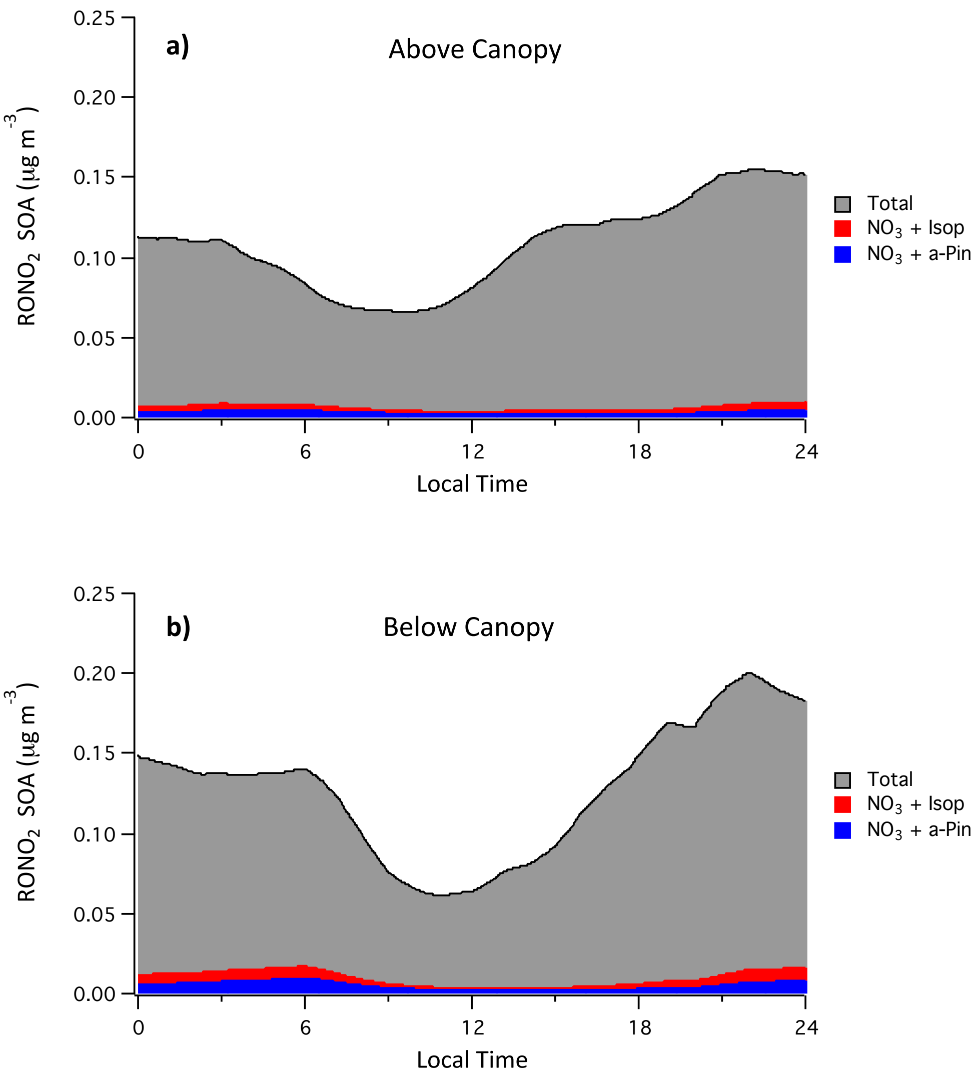

Figure S12. Diurnal profile of total $RONO_2$ SOA **(a)** above-canopy and **(b)** below-canopy including the specific contributions from NO_3 oxidation of isoprene and α-pinene.

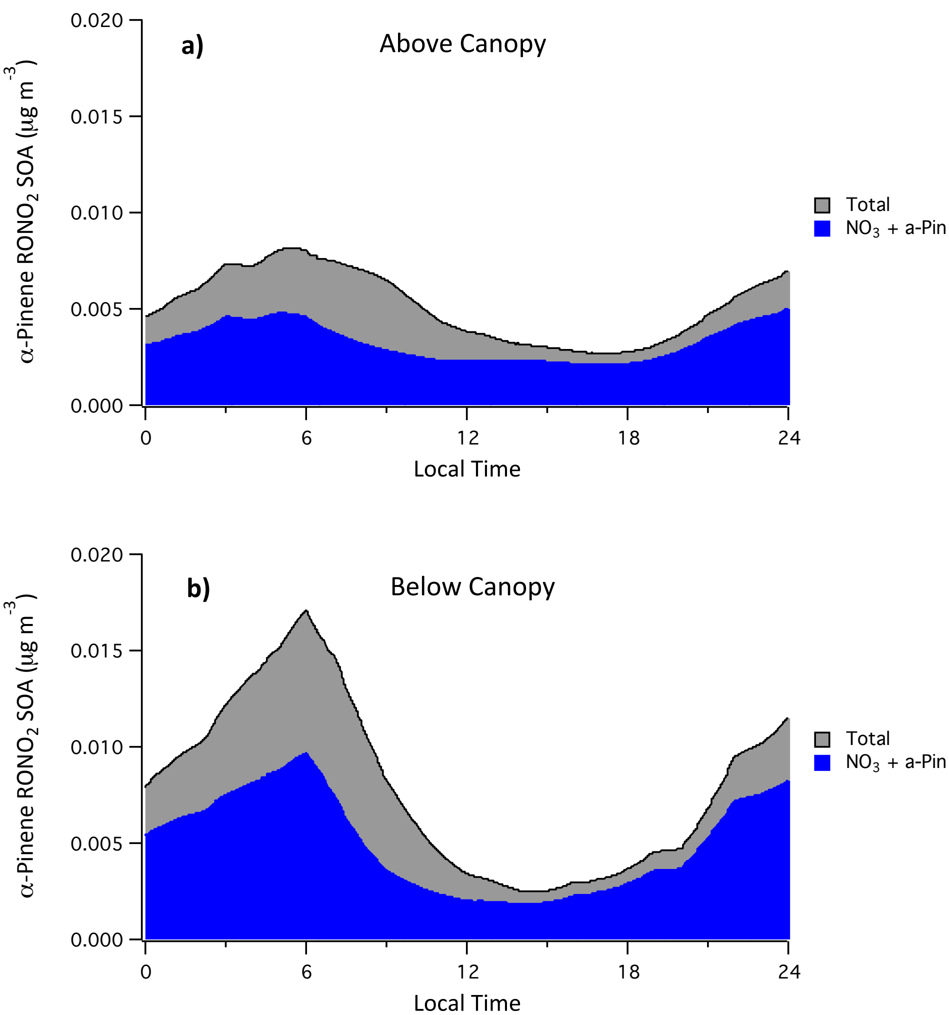

Figure S13. Contribution of NO_3 oxidation to total α-pinene $RONO_2$ SOA mass above **(a)** and below **(b)** the canopy.

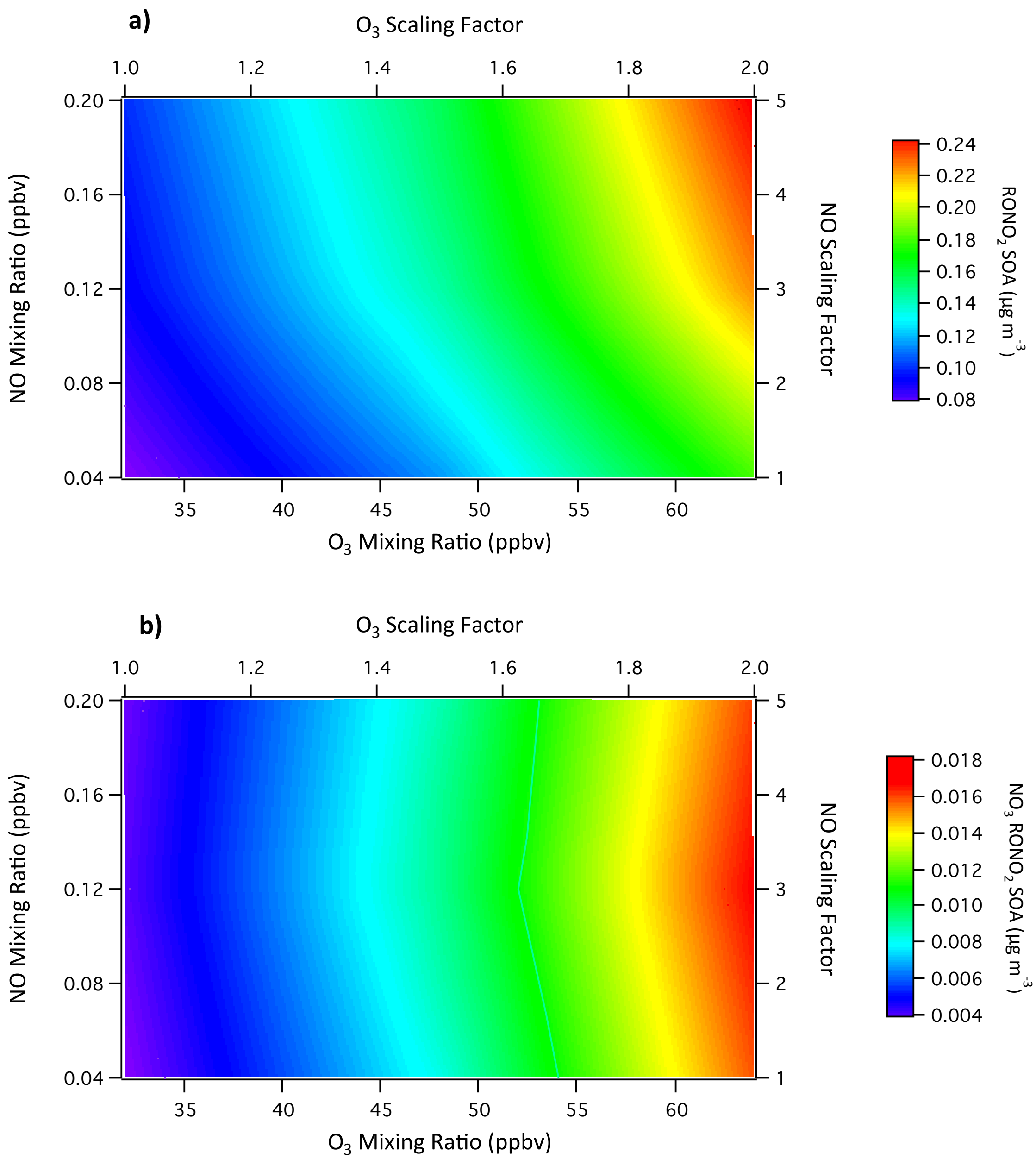

Figure S14. Mass loading of **(a)** $RONO_2$ SOA and **(b)** NO_3-derived $RONO_2$ SOA below the canopy as a function of O_3 and NO mixing ratios. Values are averages from 11:00-15:00.

Works Cited:

Ashworth, K., Chung, S. H., Griffin, R. J., Chen, J., Forkel, R., Bryan, A. M., and Steiner, A. L.: FORest Canopy Atmosphere Transfer (FORCAsT) 1.0: a 1-D model of biosphere-atmosphere chemical exchange, Geosci. Model Dev., 8, 3765-3784, doi:10.5194/gmd-8-3765-2015, 2015.

Karl, T., Harley, P., Emmons, L., Thornton, B., Guenther, A., Basu, C., Turnipseed, A., and Jardine, K.: Efficient atmospheric cleansing of oxidized organic trace gases by vegetation, Science, 330, 6005, 816–819, doi:10.1126/science.1192534, 2010.

Nguyen, T. B., Crounse, J. D., Teng, A. P., Clair, J. M. S., Paulot, F., Wolfe, G. M., and Wennberg, P. O.: Rapid deposition of oxidized biogenic compounds to a temperate forest, P. Natl. Acad. Sci. USA, 112, E392–E40, doi:10.1073/pnas.1418702112, 2015.

Sander R.: Compilation of Henry's Law Constants for Inorganic and Organic Species of Potential Importance in Environmental Chemistry (Max Planck Inst Chem, Mainz, Germany), 1999.